

Flux-averaging Analysis of Type Ia Supernova Data

Yun Wang¹
Princeton University Observatory
Peyton Hall, Princeton, NJ 08544
email: ywang@astro.princeton.edu

Abstract

Because of flux conservation, flux-averaging *justifies* the use of the distance-redshift relation for a smooth universe in the analysis of type Ia supernova (SN Ia) data. We have combined the SN Ia data from the High- z SN Search and the Supernova Cosmology Project, and binned the combined data by flux-averaging in redshift intervals of $\Delta z = 0.05$ and $\Delta z = 0.1$. We find that the unbinned data yield a Hubble constant of $H_0 = 65 \pm 1 \text{ km s}^{-1} \text{ Mpc}^{-1}$ (statistical error only), a matter density fraction of $\Omega_m = 0.7 \pm 0.4$, and a vacuum energy density fraction of $\Omega_\Lambda = 1.2 \pm 0.5$. The binned data for $\Delta z = 0.1$ yield $H_0 = 65 \pm 1 \text{ km s}^{-1} \text{ Mpc}^{-1}$ (statistical error only), $\Omega_m = 0.3 \pm 0.6$, and $\Omega_\Lambda = 0.7 \pm 0.7$. Our results are not sensitive to the redshift bin size. Flux-averaging leads to less biased estimates of the cosmological parameters by reducing the bias due to systematic effects such as weak lensing.

Comparison of the data of 18 SNe Ia published by both groups yields a mean SN Ia peak absolute magnitude of $M_B = -19.33 \pm 0.25$. The internal dispersion of each data set is about 0.20 magnitude in the *calibrated* SN Ia peak absolute magnitudes. The difference in analysis techniques introduces an additional uncertainty of about 0.15 magnitude.

If the SNe Ia peak absolute luminosity changes with redshift due to evolution, our ability to measure the cosmological parameters from SN Ia data will be significantly diminished. Assuming power-law evolution in the peak absolute luminosity, $(1+z)^\beta$, we find a strong degeneracy between the evolution power-law index β and the matter density fraction Ω_m . For $\Omega_m = 0.3$, we find that the unbinned data yields $H_0 = 65 \pm 1 \text{ km s}^{-1} \text{ Mpc}^{-1}$ (statistical error only), $\Omega_\Lambda = 1.4 \pm 1.1$, and $\beta = 0.5 \pm 1.6$, and the binned data (with $\Delta z = 0.1$) yields $H_0 = 65 \pm 1 \text{ km s}^{-1} \text{ Mpc}^{-1}$ (statistical error only), $\Omega_\Lambda = 0.6 \pm 1.4$, and $\beta = 0.0 \pm 1.0$.

¹Present address: Dept. of Physics, 225 Nieuwland Science Hall, University of Notre Dame, Notre Dame, IN 46556-5670. email: Yun.Wang.92@nd.edu

1. Introduction

Near the end of the millennium, cosmology has become a data-driven science. We are closer than ever to determining the fundamental cosmological parameters which describe our observable universe (Bahcall et al. 1999, Eisenstein, Hu, & Tegmark 1999, Turner & Tyson 1999, Wang, Spergel, & Strauss 1999). The use of astrophysical standard candles provides a fundamental means of measuring the cosmological parameters H_0 (current expansion rate of the universe), Ω_m (matter density fraction of the universe), and Ω_Λ (vacuum energy density fraction of the universe).

Type Ia supernovae (SNe Ia) are currently our best candidates for standard candles. They can be calibrated to have small intrinsic dispersions (Phillips 1993, Riess, Press, & Kirshner 1995). Two independent teams, the High- z SN Search (Schmidt et al.) and the Supernova Cosmology Project (Perlmutter et al.), have observed about 100 SNe Ia. The data analysis results of both teams seem to suggest that our universe has a significant vacuum energy content (Garnavich et al. 1998, Riess et al. 1998, Perlmutter et al. 1999).

In this paper, we combine the data of the High- z SN Search team and the Supernova Cosmology Project, and bin the combined data by flux-averaging in redshift intervals. Previous work (Wang 2000) has shown that flux-averaging is effective in reducing the scatter in SN Ia peak absolute luminosity due to weak gravitational lensing and intrinsic dispersions. Here, we study the effect of flux-averaging on the estimation of cosmological parameters. In §2 we compare the data sets from the two teams. In §3 we describe how we combine the data from the two teams. In §4 we flux-average the combined data and derive estimated cosmological parameters. In §5 we illustrate the effect of evolution of SN peak absolute luminosity on the estimation of cosmological parameters. §6 contains a summary.

2. Comparison of data sets

The published data of the High- z SN Search team (Schmidt et al. 1998, Riess et al. 1998) consists of 50 SNe Ia. They give measured distance modulus for each SN Ia, μ_0 , to be compared with the theoretical prediction

$$\mu_0^p = 5 \log \left(\frac{d_L}{\text{Mpc}} \right) + 25, \quad (1)$$

where $d_L(z)$ is the luminosity distance; it is related to the angular diameter distance $d_A(z)$ and comoving distance $r(z)$:

$$d_L(z) = (1+z)^2 d_A(z) = (1+z) r(z), \quad (2)$$

assuming a completely smooth universe.

The comoving distance $r(z)$ is given by (Weinberg 1972)

$$r(z) = \frac{cH_0^{-1}}{|\Omega_k|^{1/2}} \text{sinn} \left\{ |\Omega_k|^{1/2} \int_0^z dz' \left[\Omega_m(1+z')^3 + \Omega_\Lambda + \Omega_k(1+z')^2 \right]^{-1/2} \right\}, \quad (3)$$

where “sinn” is defined as sinh if $\Omega_k > 0$, and sin if $\Omega_k < 0$. If $\Omega_k = 0$, the sinn and Ω_k ’s disappear from Eq.(3), leaving only the integral.

The published data of the Supernova Cosmology Project (Perlmutter et al. 1999) consists of 60 SNe Ia. They give the estimated effective B-band magnitude of each SN Ia, to be compared with

$$m_B^{eff} = M_B + \mu_0^p, \quad (4)$$

where M_B is the peak absolute magnitude of a “standard” SN Ia in the B-band, and μ_0^p is given by Eq.(1).

We find that the published data of the two teams have 18 SNe Ia in common. The two data sets for the same SNe Ia should differ by the constant offset M_B . We find

$$M_B^{MLCS} \equiv m_B^{eff} - \mu_0^{MLCS} = -19.33 \pm 0.25, \quad (5)$$

$$M_B^{m15} \equiv m_B^{eff} - \mu_0^{m15} = -19.42 \pm 0.27, \quad (6)$$

where μ_0^{MLCS} and μ_0^{m15} for each SN Ia are estimated using the MLCS method and the template-fitting method (m15) respectively by Riess et al. (1998). The difference in the data from the two teams has a dispersion of about 0.25 magnitudes. This is surprisingly large since 16 of these SNe Ia were drawn from the Hamuy et al. (1996) data. For these 16 SNe Ia, we find $m_B^{eff} - \mu_0^{MLCS} = -19.30 \pm 0.24$, and $m_B^{eff} - \mu_0^{m15} = -19.40 \pm 0.26$. For the rest of this section, we only consider these 16 SNe Ia.

The simplest way to calibrate SNe Ia is to use the linear relation between maximum peak luminosity and decline time found by Phillips (1993). Hamuy et al. (1996) found $M_{max}^B = a + b[\Delta m_{15}(B) - 1.1]$, with $a = -19.258(0.048)$ and $b = 0.784(0.182)$ for 26 “low extinction” SNe Ia. Table 1 lists 16 SNe Ia from Hamuy et al. (1996) data that have been reanalyzed by both Riess et al. (1998) and Perlmutter et al. (1999).

In Table 1, M_B^{H96} is the *corrected* B band peak absolute magnitude given by Hamuy et al. (1996):

$$M_B^{H96} \equiv M_{max}^B + 5 \log(H_0/65) - 0.784(\Delta m_{15} - 1.1). \quad (7)$$

We find that for the 16 SNe Ia listed, $M_B^{H96} = -19.253 \pm 0.190$.

From Table 1, we find

$$\begin{aligned} (m_B^{eff} - \mu_0^{MLCS}) - M_B^{H96} &= -0.047 \pm 0.270 \\ (m_B^{eff} - \mu_0^{m15}) - M_B^{H96} &= -0.144 \pm 0.229. \end{aligned} \quad (8)$$

Table 1: 16 SNe Ia from Hamuy et al. (1996)

SN Ia	z	M_B^{H96}	$m_B^{eff} - \mu_0^{MLCS}$	$m_B^{eff} - \mu_0^{m15}$	$\mu_0^{MLCS} - \mu_0^p$	$\mu_0^{m15} - \mu_0^p$	$m_B^{eff} - \mu_0^p$
1990af	0.050	-19.31	-18.90	-19.04	-0.39	-0.25	-19.29
1992P	0.026	-19.16	-19.68	-19.51	0.31	0.14	-19.37
1992ae	0.075	-19.21	-19.37	-19.34	-0.05	-0.08	-19.42
1992ag	0.026	-19.05	-19.09	-19.25	-0.08	0.08	-19.17
1992al	0.014	-19.48	-19.45	-19.66	-0.16	0.05	-19.61
1992aq	0.101	-19.17	-19.25	-19.17	-0.14	-0.22	-19.39
1992bc	0.020	-19.46	-19.69	-19.59	0.00	-0.10	-19.69
1992bg	0.035	-19.40	-19.60	-19.83	0.14	0.37	-19.46
1992bh	0.045	-18.85	-19.30	-19.26	0.23	0.19	-19.07
1992bl	0.043	-19.45	-19.07	-19.34	-0.32	-0.05	-19.39
1992bo	0.018	-19.22	-19.11	-19.27	0.08	0.24	-19.03
1992bp	0.080	-19.57	-19.38	-19.69	-0.35	-0.04	-19.73
1992br	0.087	-19.12	-18.93	-18.81	0.01	-0.11	-18.92
1992bs	0.064	-18.98	-19.37	-19.39	0.12	0.14	-19.25
1993O	0.052	-19.32	-19.49	-19.77	0.02	0.30	-19.47
1993ag	0.050	-19.27	-19.11	-19.42	-0.12	0.19	-19.23

This indicates that the absolute magnitude of a “standard” SN Ia derived from comparing the Riess et al. (1998) and the Perlmutter et al. (1999) data sets differs appreciably from that derived by Hamuy et al. (1996) from the same 16 SNe Ia.

To account for these differences, we examine the internal dispersion of each data set. Using μ_0^p from Eq.(1) with $z \ll 1$ and $H_0 = 65 \text{ km s}^{-1} \text{ Mpc}^{-1}$, we find

$$\begin{aligned}
 \mu_0^{MLCS} - \mu_0^p &= -0.043 \pm 0.195 \\
 \mu_0^{m15} - \mu_0^p &= 0.054 \pm 0.178 \\
 m_B^{eff} - \mu_0^p &= -19.34 \pm 0.22
 \end{aligned}
 \tag{9}$$

These should be compared with $M_B^{H96} = -19.253 \pm 0.190$ for the 16 SNe Ia calibrated using Eq.(7). Fig.1 shows the internal dispersions in the calibrated SN Ia peak absolute magnitudes, as given by (a) $\mu_0^{MLCS} - \mu_0^p$, (b) $\mu_0^{m15} - \mu_0^p$, (c) $m_B^{eff} - \mu_0^p$, and (d) M_B^{H96} . Clearly, the internal dispersion for each data set is about $\sigma_{int} \sim 0.20$ magnitude. This indicates that these 16 SNe Ia can be calibrated to be standard candles with a dispersion (intrinsic and observational) of about 0.2 magnitude.

Next, we examine how the difference in analysis techniques introduces uncertainty. For the Riess et. al 1998 data analyzed using MLCS method and template-fitting method

respectively, we find

$$\mu_0^{MLCS} - \mu_0^{m15} = -0.097 \pm 0.163. \quad (10)$$

For the Perlmutter et al. (1999) data and the Hamuy et al. (1996) data, we find

$$(m_B^{eff} - \mu_0^p) - M_B^{H96} = -0.09 \pm 0.147. \quad (11)$$

It seems that the difference in analysis technique typically introduces a uncertainty of $\sigma_{tech} \sim 0.15$ magnitude.

Therefore, the difference between independently analyzed data sets could be as large as $\sigma = \sqrt{\sigma_{int}^2 + \sigma_{tech}^2} \sim 0.25$. The differences between the Riess et al. (1998) data and the Perlmutter et al. (1999) data stem mostly from the internal dispersion in the peak absolute magnitudes of SNe Ia estimated from each data set, with a substantial contribution from the difference in analysis techniques.

Eq.(8) indicates that the SN Ia absolute magnitude estimated using $m_B^{eff} - \mu_0^{MLCS}$ is closer to that found by Hamuy et al. (1996). We will use the MLCS method data from Riess et al. (1998) for the rest of this paper.

3. Combination of Data

We combine the data from the two teams by adding 42 SNe Ia from the Supernova Cosmology Project to the High- z SN Search data (the MLCS method results), leaving out the 18 SNe Ia from the Supernova Cosmology Project which are already included in the High- z SN Search data. This yields a combined data set of 92 SNe Ia. In the combined data set, we convert m_B^{eff} of the the SNe Ia which have been taken from the Supernova Cosmology Project to μ_0^{MLCS} by using Eq.(4) with $M_B = -19.33$. $M_B = -19.33$ is the mean difference in the data ($m_B^{eff} - \mu_0^{MLCS}$) of the 18 SNe Ia published by both teams [see Eq.(5)]. Fig.2 shows the difference between m_B^{eff} and μ_0^{MLCS} for these 18 SNe Ia.

Fig.3 shows the magnitude-redshift plots of the combined data set of 92 SNe Ia. The solid points represent 50 SNe Ia from Schmidt et al. data. The circles represent 42 additional SNe Ia from Perlmutter et al. The dashed line is the prediction of the open cold dark matter model (OCDM) with $\Omega_m = 0.2$ and $\Omega_\Lambda = 0$. The dotted line is the prediction of the standard cold dark matter model (SCDM) with $\Omega_m = 1$ and $\Omega_\Lambda = 0$. The two thick solid lines are flat models with a cosmological constant (Λ CDM): $(\Omega_m, \Omega_\Lambda) = (0.3, 0.7)$ and $(\Omega_m, \Omega_\Lambda) = (0.2, 0.8)$. The thin solid line is the SCDM model $(\Omega_m, \Omega_\Lambda) = (1, 0)$ with $(1+z)$ dimming of SN Ia peak luminosity (linear evolution). Fig.3(a) shows the distance modulus versus redshift. Fig.3(b) shows the distance modulus relative to the prediction of the OCDM model.

3.1. Estimation of the cosmological parameters

We find that the best-fit values of the cosmological parameters are sensitive to the estimated errors of the data points. Following Riess et al. (1998), we use

$$\chi^2(H_0, \Omega_m, \Omega_\Lambda) = \sum_i \frac{[\mu_{0,i}^p(z_i|H_0, \Omega_m, \Omega_\Lambda) - \mu_{0,i}]^2}{\sigma_{\mu_0,i}^2 + \sigma_{mz,i}^2}, \quad (12)$$

where σ_{μ_0} is the estimated measurement error of the distance modulus, and σ_{mz} is the dispersion in the distance modulus due to the dispersion in galaxy redshift, σ_z , due to peculiar velocities and uncertainty in the galaxy redshift (for the Perlmutter et al. data, the dispersion due to peculiar velocities is included in $\sigma_{m_B^{eff}}$, i.e., σ_{μ_0}). Since

$$\sigma_{mz} = \frac{5}{\ln 10} \left(\frac{1}{d_L} \frac{\partial d_L}{\partial z} \right) \sigma_z, \quad (13)$$

σ_{mz} depends on Ω_Λ and Ω_m . We compute σ_{mz} iteratively while estimating the cosmological parameters.

For the Schmidt et al. data, we follow Riess et al. (1998) in adopting $\sigma_z = 200 \text{ km s}^{-1}$, and add 2500 km s^{-1} in quadrature to σ_z for SNe Ia whose redshifts were determined from broad features in the SN spectrum. For the Perlmutter et al. data, we take $\sigma_{\mu_0} = \sigma_{m_B^{eff}}$, which already includes dispersion due to peculiar velocities of 300 km s^{-1} , and we use the redshift uncertainty σ_z for each SN Ia given in their tables to compute σ_{mz} (see Eq.(13)).

Table 2 lists the derived best-fit cosmological parameters, with $1\text{-}\sigma$ error bars, for the High- z SN Search data (Schmidt et al.), the Supernova Cosmology Project data (Perlmutter et al.), and the combined data. Note that h is the dimensionless Hubble constant, defined by $H_0 = 100 h \text{ km s}^{-1} \text{ Mpc}^{-1}$. χ_ν^2 is χ^2 per degree of freedom.

Fig.4 shows the 68.3% and 95.4% confidence contours in the $\Omega_\Lambda - \Omega_m$ plane. The dotted lines represent the Schmidt et al. data (50 SNe Ia), the dashed lines represent the Perlmutter et al. data (60 SNe Ia), and the solid lines represent the combined data (92 SNe Ia). Note that we have allowed Ω_m to be a free parameter in estimating its value. Since distances are *not* directly measurable, we can treat them as theoretical intermediaries in the data analysis, therefore Ω_m must be allowed to have negative as well as positive and zero values, for statistical robustness.

We have combined data from two independent teams analyzed using different statistical methods. It is important to analyze all the SN data with the same techniques for statistical consistency; this is not possible at present, because not all the reduced SN Ia data have become public (Perlmutter et al. have not yet published the light curves of their 42 SNe Ia). However, the published data from the two teams are similar enough (with a constant offset) to allow a meaningful study of the effect of flux-averaging on the estimation of cosmological parameters from SN Ia data (see §4 and §5).

Table 2: Estimated cosmological parameters with SNe Ia

	50 SNe Ia (Schmidt et al.)	60 SNe Ia (Perlmutter et al.)	92 SNe Ia (combined data)
h	$0.65 \pm 0.01^*$	$0.66 \pm 0.02^*$	$0.65 \pm 0.01^*$
Ω_m	0.2 ± 0.6	1.0 ± 0.4	0.7 ± 0.4
Ω_Λ	0.7 ± 0.8	1.7 ± 0.6	1.2 ± 0.5
χ_ν^2	1.16	1.63	1.48

Note. — *Statistical error only, not including the contribution from the much larger SN Ia absolute magnitude error.

3.2. H_0 as a systematic indicator of data sets

We have chosen to estimate H_0 simultaneously with Ω_m and Ω_Λ mainly for three reasons.

First, H_0 is a useful indicator of the systematic “zero point” of a given SN Ia data set. Let us consider the 16 SNe Ia from Hamuy et al. (1996) that both teams (Riess et al. 1998, Perlmutter et al. 1999) have reanalyzed (see §2). Since each of these 16 SNe Ia can only have one true peak absolute magnitude, we take $M_B^{MLCS} = M_B^{eff} = M_B^{H96}$, where M_B^{MLCS} , M_B^{eff} , and M_B^{H96} are the peak absolute magnitudes derived from the Riess et al. 1998 (MLCS), Perlmutter et al. 1999, and Hamuy et al. 1996 data respectively. From Eq.(9), $\mu_0^{MLCS} - \mu_0^p = -0.043$ and $m_B^{eff} - \mu_0^p = -19.34$. Using $m_B^{eff} = M_B^{eff} + \mu_0^{eff}$, and setting $M_B^{eff} = M_B^{H96} = -19.253$, we find $\mu_0^{eff} - \mu_0^p = -0.087$. Hence

$$\mu_0^{MLCS} - \mu_0^{eff} = -\frac{5}{\ln 10} \frac{\Delta H_0}{H_0} = 0.044, \quad (14)$$

i.e., the difference between the estimated values for the Hubble constant from Riess et al. 1998 (H_0^{MLCS}) and Perlmutter et al. 1999 (H_0^{eff}) data is

$$H_0^{MLCS} - H_0^{eff} = -1.32, \quad (15)$$

for $H_0^{MLCS} = 65$. This is in agreement with the estimated values of H_0 listed in Table 2 for 50 SNe Ia from the Riess et al. (1998) data and for 60 SNe Ia from the Perlmutter et al. (1999) data. The SNe Ia from Perlmutter et al. (1999) are systematically brighter than the Riess et al. (1998) SNe Ia by about 0.04 magnitude.

Second, integrating out the H_0 dependence in the probability distribution functions of the cosmological parameters have very little effect on the estimated values of Ω_m and Ω_Λ ,

because the H_0 dependence is uncorrelated with the Ω_m and Ω_Λ dependence. Therefore, we have little to gain in the accuracy of estimated Ω_m and Ω_Λ by excluding H_0 from the parameter estimation.

Third, including H_0 in the parameter estimation conforms with the common practice of estimating all basic cosmological parameters simultaneously when analyzing other cosmological data sets, for example, the Cosmic Microwave Background Anisotropy data (Wang, Spergel, & Strauss 1999, Eisenstein, Hu, & Tegmark 1999). The distance modulus depends on H_0 , as well as Ω_m and Ω_Λ . Therefore, H_0 should be estimated from the SNe Ia data simultaneously with Ω_m and Ω_Λ , although the H_0 dependence of the data is independent of the dependence on Ω_m and Ω_Λ .

To summarize, including H_0 in the cosmological parameter estimation from SN Ia data provides a useful systematic indicator of the data set used, while having little effect on the accuracy of the other cosmological parameters (Ω_m and Ω_Λ) being estimated, and it conforms with the convention used in parameter estimation from other cosmological data. Note that the error of the H_0 estimated here only reflects statistical error, it does not include the contribution from the much larger SN Ia peak absolute magnitude error. For a realistic assessment of the actual value and errors associated with H_0 estimated from SNe Ia, the reader is referred to Saha et al. (1999), Jha et al. (1999), and Gibson et al. (1999).

4. Flux-averaging of data

An important reason to consider flux-averaging is the weak gravitational lensing of SNe Ia. Because our universe is inhomogeneous in matter distribution, weak gravitational lensing leads to a non-Gaussian distribution in the magnification of standard candles.

For a given redshift z , if a mass-fraction $\tilde{\alpha}$ of the matter in the universe is smoothly distributed, the largest possible distance for light bundles which have not passed through a caustic is given by the solution to the Dyer-Roeder equation (Dyer & Roeder 1973, Schneider et al. 1992, Kantowski 1998):

$$g(z) \frac{d}{dz} \left[g(z) \frac{dD_A}{dz} \right] + \frac{3}{2} \tilde{\alpha} \Omega_m (1+z)^5 D_A = 0,$$

$$D_A(z=0) = 0, \quad \left. \frac{dD_A}{dz} \right|_{z=0} = \frac{c}{H_0}, \quad (16)$$

where $g(z) \equiv (1+z)^3 \sqrt{1 + \Omega_m z + \Omega_\Lambda [(1+z)^{-2} - 1]}$. The smoothness parameter $\tilde{\alpha}$ essentially represents the amount of matter that can cause the magnification of a given source. If we define a direction-dependent smoothness parameter $\tilde{\alpha}$ via the Dyer-Roeder equation, there is a unique mapping between $\tilde{\alpha}$ and the magnification of a source. We can think of our universe as a mosaic of cones centered on the observer, each with a

different value of $\tilde{\alpha}$. Wang (1999) has derived empirical fitting formulae for the probability distribution of $\tilde{\alpha}$ from the numerical simulation results of Wambsganss et al. (1997).

Wang (2000) showed that flux-averaging of simulated data (with noise due to both weak lensing and intrinsic dispersions) leads to SN peak luminosities which well approximate the true luminosities with $\tilde{\alpha} = 1$ (which represents a completely smooth universe). The angular-diameter distance defined in Eq.(2) using the comoving distance $r(z)$, $d_A(z) = r(z)/(1+z)$, satisfies Eq.(16) with $\tilde{\alpha} = 1$, i.e., the angular-diameter distance defined in Eq.(2) is the Dyer-Roeder distance with $\tilde{\alpha} = 1$. Therefore, flux-averaging *justifies* the use of Eq.(2) in the analysis of SN Ia data.

Before flux-averaging, we convert the distance modulus of SNe Ia into “fluxes”, $f(z_i) = 10^{-\mu_0(z_i)/2.5}$. We then obtain “absolute luminosities”, $\{\mathcal{L}(z_i)\}$, by removing the redshift dependence of the “fluxes”, i.e.,

$$\mathcal{L}(z_i) = 4\pi d_L^2(z_i|H_0, \Omega_m, \Omega_\Lambda) f(z_i), \quad (17)$$

where d_L is the luminosity distance, and $(H_0, \Omega_m, \Omega_\Lambda)$ are the best-fit cosmological parameters derived from the unbinned data set $\{f(z_i)\}$. We then flux-average over the “absolute luminosities” $\{\mathcal{L}_i\}$ in each redshift bin. The set of best-fit cosmological parameters derived from the binned data is applied to the unbinned data $\{f(z_i)\}$ to obtain a new set of “absolute luminosities” $\{\mathcal{L}_i\}$, which is then flux-averaged in each redshift bin, and the new binned data is used to derive a new set of best-fit cosmological parameters. This procedure is repeated until convergence is achieved. The $1-\sigma$ error on each binned data point is taken to be the root mean square of the $1-\sigma$ errors on the unbinned data points in the given redshift bin, $\{f_i\}$ ($i = 1, 2, \dots, N$), multiplied by $1/\sqrt{N}$ (see Wang 2000).

Fig.5 shows magnitude-redshift plots of the binned data for the total of 92 SNe Ia, with redshift bin $\Delta z = 0.05$. The lines are the same as in Fig.1. Fig.5(a) shows the distance modulus versus redshift. Fig.5(b) shows the distance modulus relative to the prediction of the open cold dark matter model (OCDM) with $\Omega_m = 0.2$ and $\Omega_\Lambda = 0$. Fig.6 is the same as Fig.5, but with redshift bin $\Delta z = 0.1$.

Table 3 lists the estimated cosmological parameters, with $1-\sigma$ error bars.

Fig.7 shows the 68.3% and 95.4% confidence contours in the $\Omega_\Lambda - \Omega_m$ plane. The solid lines represent the unbinned data, the dotted lines represent the binned data with redshift bin $\Delta z = 0.05$; the dashed lines represent the binned data with redshift bin $\Delta z = 0.1$.

Fig.8 shows that the estimated parameters from flux-averaged data are not sensitive to the size of the redshift bin. The thick solid lines are the estimated Ω_m (a) and Ω_Λ (b) as functions of the redshift bin size dz , the dotted lines mark the 1σ errors on Ω_m (a) and Ω_Λ (b). The thin solid line is $\chi_\nu^2 + 2$. The wiggles in the lines are due to the small number of SNe Ia in each redshift bin for small bin size, and due to the small number of binned data points for large bin size. Clearly, the optimal range for the bin size is $0.025 \lesssim dz \lesssim 0.9$.

Table 3: Estimated cosmological parameters with 92 SNe Ia

N_{data}	unbinned data 92	binned with $\Delta z = 0.05$ 17	binned with $\Delta z = 0.1$ 10
h	$0.65 \pm 0.01^*$	$0.65 \pm 0.01^*$	$0.65 \pm 0.01^*$
Ω_m	0.7 ± 0.4	0.3 ± 0.6	0.3 ± 0.6
Ω_Λ	1.2 ± 0.5	0.7 ± 0.7	0.7 ± 0.7
χ^2_ν	1.48	0.73	0.78
fixing $\Omega_\Lambda = 1 - \Omega_m$			
h	$0.65 \pm 0.01^*$	$0.65 \pm 0.01^*$	$0.65 \pm 0.01^*$
Ω_m	0.3 ± 0.1	0.3 ± 0.1	0.3 ± 0.1
χ^2	1.47	0.68	0.68
fixing $\Omega_\Lambda = 0$			
h	$0.64 \pm 0.01^*$	$0.65 \pm 0.01^*$	$0.65 \pm 0.01^*$
Ω_m	-0.2 ± 0.1	-0.2 ± 0.1	-0.2 ± 0.1
χ^2	1.49	0.72	0.76
fixing $\Omega_m = 0.3$			
h	$0.65 \pm 0.01^*$	$0.65 \pm 0.01^*$	$0.65 \pm 0.01^*$
Ω_Λ	0.7 ± 0.1	0.7 ± 0.2	0.7 ± 0.2
χ^2	1.47	0.68	0.68

Note. — *Statistical error only, not including the contribution from the much larger SN Ia absolute magnitude error.

Because flux-averaging reduces the bias due to weak lensing, the flux-averaged data yield less biased estimates of the cosmological parameters.

5. Effect of evolution

Drell, Loredo, & Wasserman (1999) have studied the effect of SN Ia luminosity evolution on the estimation of cosmological parameters. Recently, Riess et al. (1999) suggested that there is an indication of evolution of SNe Ia from their risetimes, and that if this observed evolution affects the peak luminosities of SNe Ia, it can account for the observed faintness of high- z SNe Ia without invoking a cosmological constant. To illustrate this interesting possibility, we introduce a power-law evolution in the SNe Ia peak

luminosity, $\mathcal{L}(z) = 4\pi d_L^2(z) f(z)$, i.e.,

$$\mathcal{L}(z) = (1+z)^\beta \mathcal{L}(z=0). \quad (18)$$

Here, $\beta > 0$ represents brightening of SN Ia with redshift, while $\beta < 0$ represents dimming with redshift. The thin solid line in Fig.3, Fig.5, and Fig.6 represent the Λ CDM model ($\Omega_m = 1, \Omega_\Lambda = 0$) with linear dimming of the SN Ia peak luminosity with $\beta = -1$.

Table 4 lists the estimated cosmological parameters and SN Ia evolution power-law index β , with 1- σ error bars, for the combined data set of 92 SNe Ia.

Table 4: Estimated cosmological parameters with SN evolution

N_{data}	unbinned data	binned with $\Delta z = 0.05$	binned with $\Delta z = 0.1$
	92	17	10
h	$0.66 \pm 0.02^*$	$0.65 \pm 0.02^*$	$0.65 \pm 0.03^*$
Ω_m	1.5 ± 5.8	0.8 ± 22.5	0.9 ± 31.3
Ω_Λ	1.2 ± 0.8	0.4 ± 4.5	0.4 ± 3.3
β	-0.7 ± 3.7	-0.6 ± 17.1	-0.6 ± 21.1
χ^2_ν	1.49	0.78	0.91
	fixing $\Omega_m = 0.3$		
h	$0.65 \pm 0.01^*$	$0.65 \pm 0.01^*$	$0.65 \pm 0.01^*$
Ω_Λ	1.4 ± 1.1	0.7 ± 1.3	0.6 ± 1.4
β	0.5 ± 1.6	0.0 ± 1.0	0.0 ± 1.0
χ^2	1.59	0.73	0.78

Note. — *Statistical error only, not including the contribution from the much larger SN Ia absolute magnitude error.

There is strong degeneracy, as expected, between the evolution power-law index β and the matter density fraction Ω_m . If the SNe Ia peak absolute luminosity changes with redshift due to evolution, our ability to measure the cosmological parameters from SN Ia data will be significantly diminished, unless we can correct for the evolution. The issue of SN evolution can only be settled if a large number of SNe Ia are observed at $z > 1$; this can be accomplished via a supernova pencil beam survey using a dedicated 4 meter telescope (Wang 2000).

6. Conclusions

We have combined the data from the two independent SN Ia groups, Schmidt et al. and Perlmutter et al., and analyzed the combined data using flux-averaging in redshift bins of 0.05 and 0.1. We find that the estimation of the cosmological parameters is not sensitive to the size of the redshift bin. While the combined data without flux-averaging are best fit by a closed universe with high matter content and larger than critical density vacuum energy, the flux-averaged data are best fit by a nearly flat universe with a low matter content. This is consistent with the strong observational evidence that we live in a low matter density universe (Bahcall, Lubin, & Dorman 1995, Carlberg et al. 1996, Bahcall & Fan 1998, Krauss 1998, Bahcall et al. 1999). Flux-averaging leads to less biased estimates of the cosmological parameters by reducing the bias due to systematic effects such as weak lensing.

The distance-redshift relation, Eq.(3), is generally used in making theoretical predictions to compare with the brightnesses of standard candles. However, it is only valid in a smooth universe. We live in a clumpy universe. Because of flux conservation, flux-averaging justifies the use of Eq.(3) in the analysis of SN Ia data (see §4).

In the estimation of cosmological parameters, we have allowed the matter density fraction Ω_m and the vacuum energy density fraction Ω_Λ to be unconstrained free parameters. Unlike fluxes, distances are *not* directly measurable, therefore they are best treated as theoretical intermediaries. Since the cosmological parameters Ω_m and Ω_Λ enter through distances [see Eqs.(2) & (3)], they should be allowed to have negative as well as positive and zero values for statistical robustness. By not applying priors on Ω_m and Ω_Λ in our parameter estimation, we can check the validity of Eqs.(2) & (3). For example, if the most probable value of Ω_m derived from the data is negative ($\Omega_m < 0$), it could be an indication that Eqs.(2) and (3) do not apply, since we know that $\Omega_m > 0$.

We have also investigated the effect of possible evolution of SNe Ia on the estimation of cosmological parameters. Assuming power-law evolution in the SN Ia peak absolute luminosity, we find that there is strong degeneracy between the evolution power-law index and the matter density in the universe. The evolution of SNe Ia must be resolved before they can be regarded as reliable standard candles. Supernova pencil beam surveys which could yield hundreds of SNe Ia at $z > 1$ over a few years will be critical in constraining the evolution of SNe Ia (Wang 2000).

Acknowledgements

It is a pleasure for me to thank Neta Bahcall for helpful comments and a careful reading of the manuscript, and the referee for useful suggestions.

REFERENCES

- Bahcall, N.A. & Fan, X. 1998, ApJ 504, 1; Nat. Acad. Sci. Proc. 95, 5956
- Bahcall, N.A., Lubin, L.M., and Dorman, V. 1995, ApJ 447, L81
- Bahcall, N.A., Ostriker, JP, Perlmutter, S., and Steinhardt, P., 1999, Science, 284, 1481
- Carlberg, R.G., Yee, H.K.C. et al. 1996, ApJ, 462, 32
- Drell, P.S.; Lored, T.J.; & Wasserman, I. 1999, astro-ph/9905027, ApJ in press
- Dyer, C.C., & Roeder, R.C. 1973, ApJ, 180, L31
- Eisenstein, D.J., Hu, W., & Tegmark, M. 1999, ApJ, 518, 2
- Garnavich, P.M. et al. 1998, ApJ, 493, L53
- Gibson, B.K. et al. 1999, astro-ph/9908149, ApJ in press
- Hamuy, M. et al. 1996, AJ, 112, 2391
- Jha, S. et al. 1999, astro-ph/9906220, ApJS in press
- Kantowski, R. 1998, ApJ, 507, 483
- Krauss, L.M. 1998, ApJ, 501, 461
- Perlmutter, S., et al. 1999, ApJ, 517, 565
- Phillips, M.M. 1993, ApJ, 413, L105
- Riess, A.G., Press, W.H., & Kirshner, R.P. 1995, ApJ, 438, L17
- Riess, A.G., et al 1998, AJ, 116, 1009
- Riess, A.G., et al. 1999, astro-ph/9907037
- Saha, A. et al. 1999, astro-ph/9904389, ApJ in press
- Schneider, P., Ehlers, J., & Falco, E.E. 1992, Gravitational Lenses, Springer-Verlag, Berlin
- Schmidt, B.P., et al. 1998, ApJ, 507, 46
- Turner, M.S., & Tyson, J.A. 1999, RvMPS, 71, 145
- Wambsganss, J., Cen, R., Xu, G., & Ostriker, J.P. 1997, ApJ, 475, L81
- Wang, Y. 1999, ApJ, 525, 651

Wang, Y. 2000, astro-ph/9806185, ApJ in press

Wang, Y., Spergel, D.N., & Strauss, M.A. 1999, ApJ, 510, 20, astro-ph/9802231

Weinberg, S. 1972, Gravitation and Cosmology, John Wiley & Sons, New York

Fig. 1.— The internal dispersions in the calibrated SN Ia peak absolute magnitudes from four data sets. (a) $\mu_0^{MLCS} - \mu_0^p$, (b) $\mu_0^{m15} - \mu_0^p$, (c) $m_B^{eff} - \mu_0^p$, and (d) M_B^{H96} .

Fig. 2.— The difference between m_B^{eff} (Perlmutter et al. 1999) and μ_0^{MLCS} (Riess et al. 1998) for the same 18 SNe Ia. The error bars are the combined errors in m_B^{eff} and μ_0^{MLCS} .

Fig. 3.— The magnitude-redshift plots of the combined data set of 92 SNe Ia. The solid points represent 50 SNe Ia from Schmidt et al. data. The empty points represent 42 additional SNe Ia from Perlmutter et al. data. The dashed line is the prediction of OCDM with $\Omega_m = 0.2$ and $\Omega_\Lambda = 0$. The dotted line is the prediction of SCDM with $\Omega_m = 1$ and $\Omega_\Lambda = 0$. The two thick solid lines are predictions of Λ CDM, with $(\Omega_m, \Omega_\Lambda) = (0.3, 0.7)$, $(\Omega_m, \Omega_\Lambda) = (0.2, 0.8)$ respectively. The thin solid line is SCDM with $(1+z)$ dimming of SN Ia peak luminosity. (a) The distance modulus versus redshift. (b) The distance modulus relative to the prediction of the OCDM model.

Fig. 4.— The 68.3% and 95.4% confidence contours in the $\Omega_\Lambda - \Omega_m$ plane. The dotted lines represent the Schmidt et al. data (50 SNe Ia), the dashed lines represent the Perlmutter et al. data (60 SNe Ia), and the solid lines represent the combined data (92 SNe Ia).

Fig. 5.— The magnitude-redshift plots of the binned data for 92 SNe Ia, with redshift bin $\Delta z = 0.05$. The line types are the same as in Fig.3. (a) The distance modulus versus redshift. (b) The distance modulus relative to the prediction of the open cold dark matter model (OCDM) with $\Omega_m = 0.2$ and $\Omega_\Lambda = 0$.

Fig. 6.— The same as Fig.5, but with redshift bin $\Delta z = 0.1$.

Fig. 7.— The 68.3% and 95.4% confidence contours in the $\Omega_\Lambda - \Omega_m$ plane. The solid lines represent the unbinned data, the dotted lines represent the binned data with redshift bin $\Delta z = 0.05$; the dashed lines represent the binned data with redshift bin $\Delta z = 0.1$.

Fig. 8.— The estimated parameters from flux-averaged data as functions of the size of the redshift bin. The thick solid line is the estimated parameter, with 1σ errors marked by the dotted lines. The thin solid line is $\chi_\nu^2 + 2$. (a) Ω_m , (b) Ω_Λ .

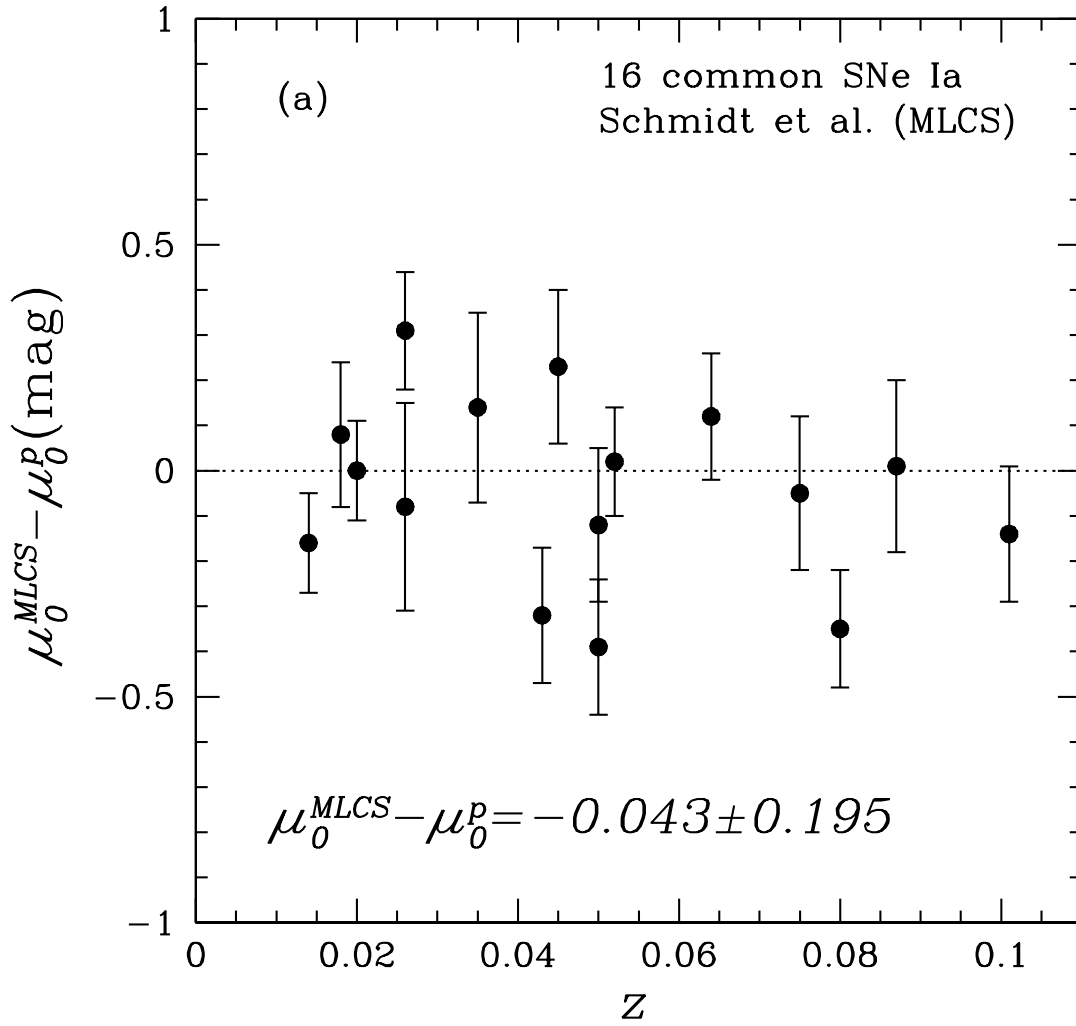


Fig. 1.— The internal dispersions in the calibrated SN Ia peak absolute magnitudes from four data sets. (a) $\mu_0^{MLCS} - \mu_0^p$.

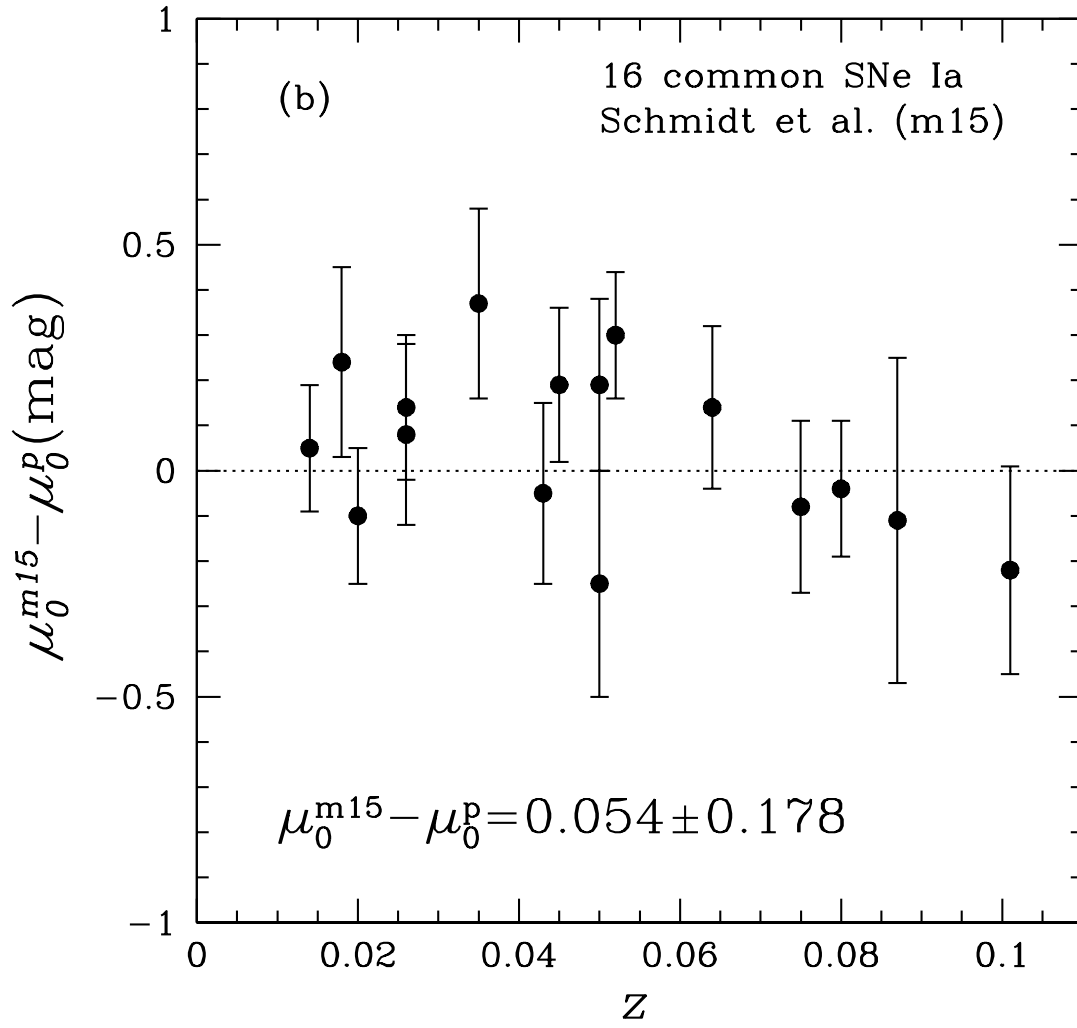


Fig. 1.— (b) $\mu_0^{m15} - \mu_0^p$.

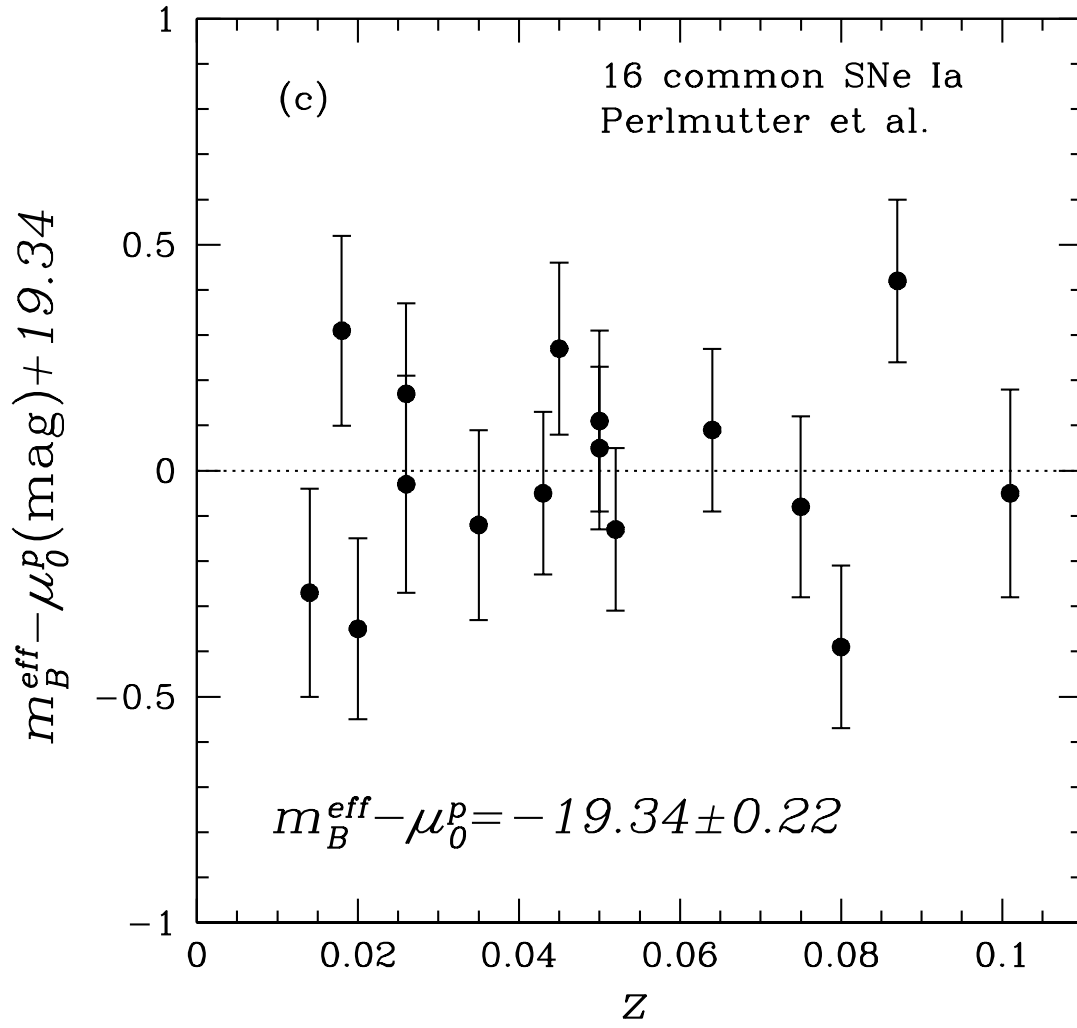


Fig. 1.— (c) $m_B^{eff} - \mu_0^p$.

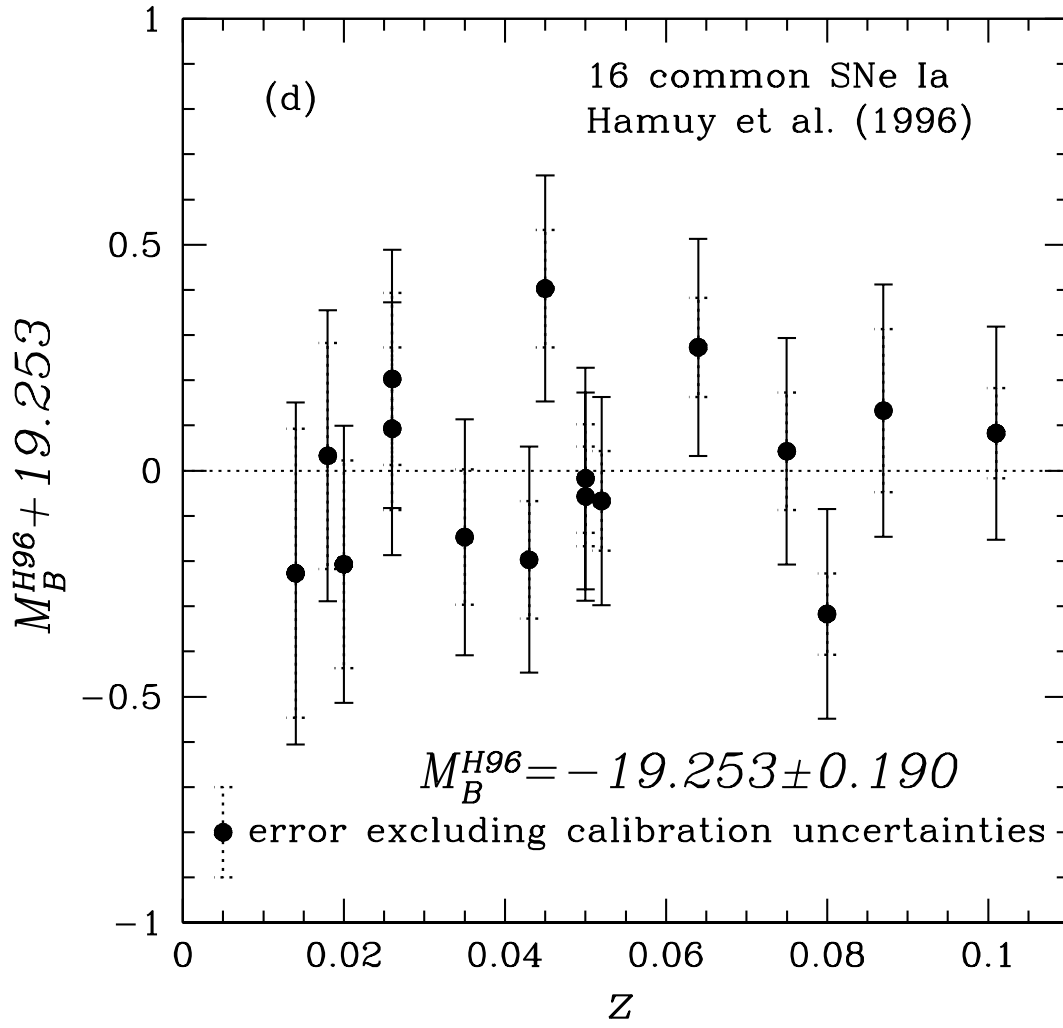


Fig. 1.— (d) M_B^{H96} .

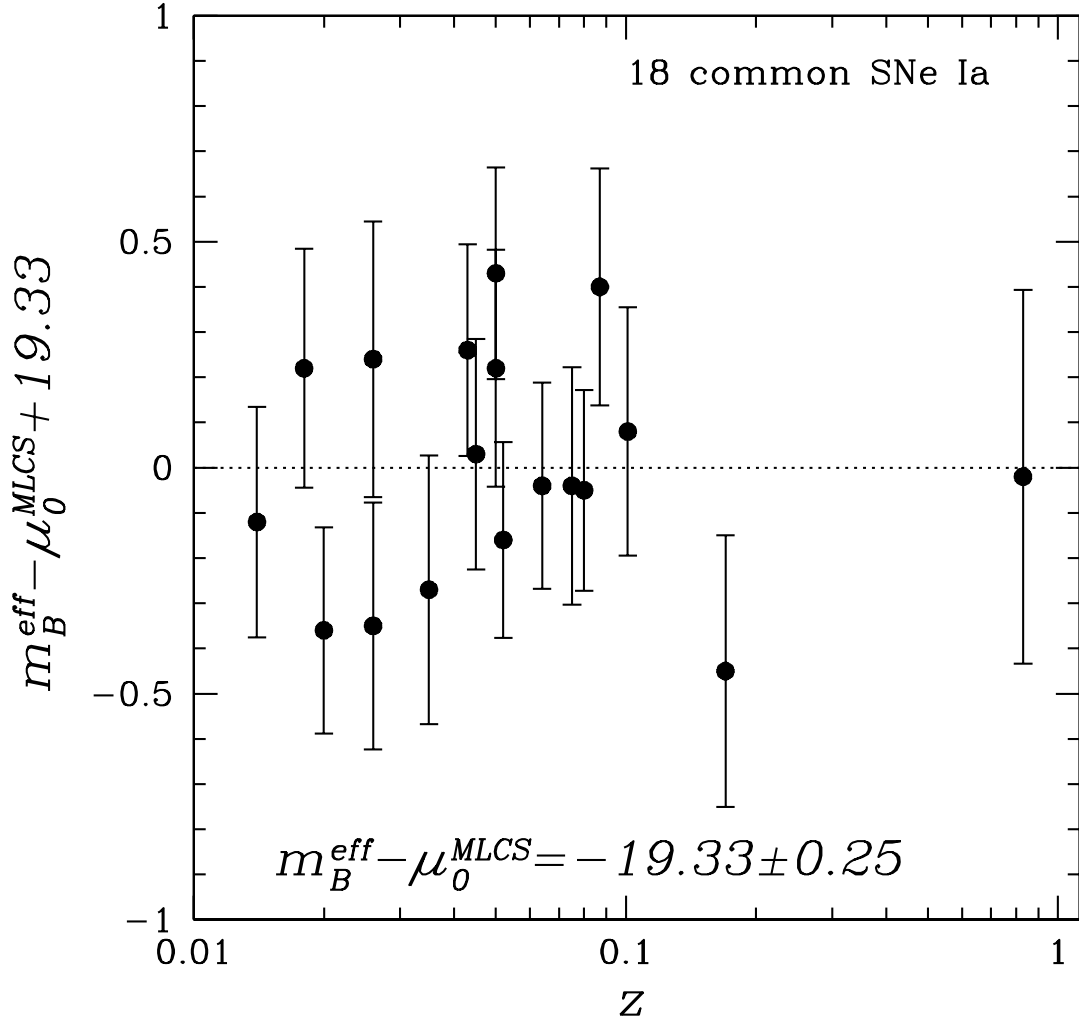


Fig. 2.— The difference between m_B^{eff} (Perlmutter et al. 1999) and μ_0^{MLCS} (Riess et al. 1998) for the same 18 SNe Ia. The error bars are the combined errors in m_B^{eff} and μ_0^{MLCS} .

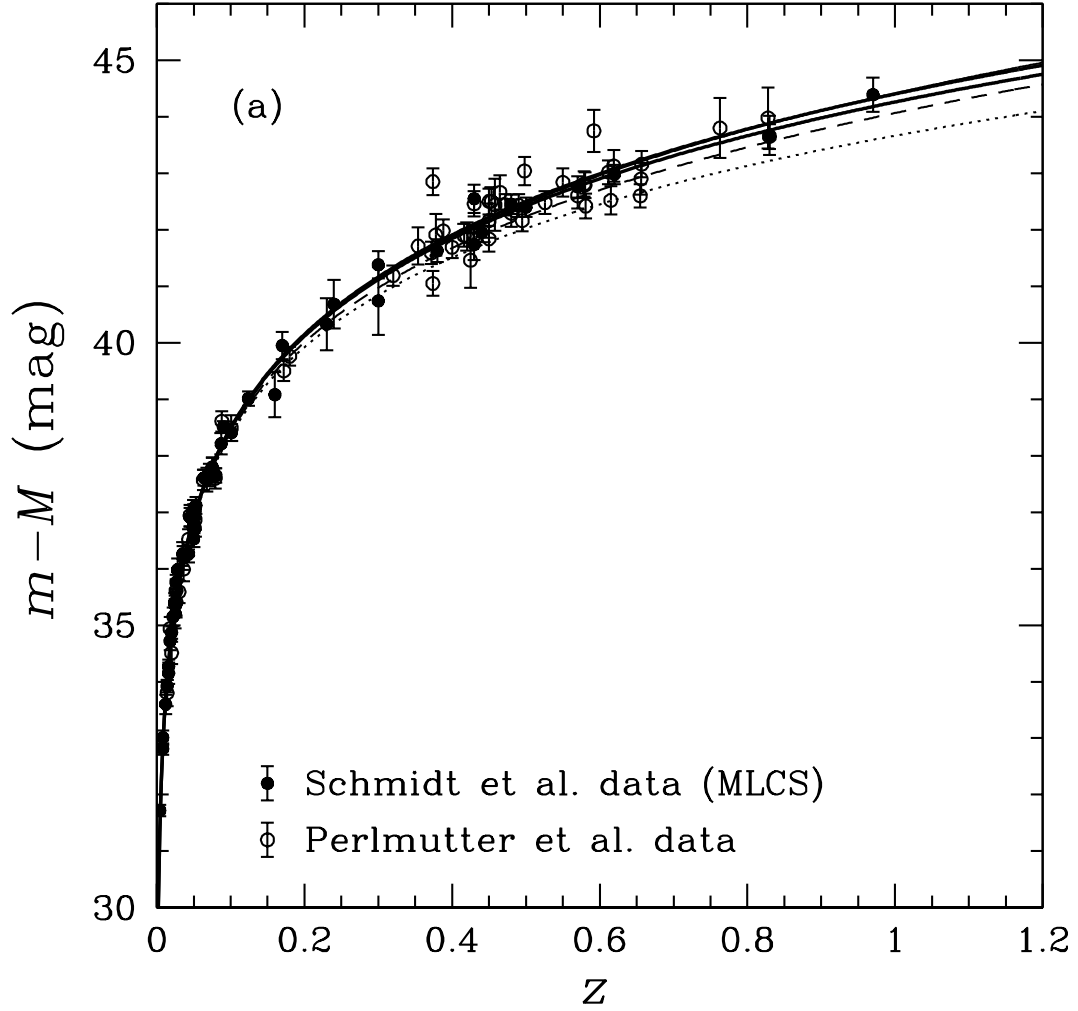


Fig. 3.— The magnitude-redshift plots of the combined data set of 92 SNe Ia. The solid points represent 50 SNe Ia from Schmidt et al. data. The empty points represent 42 additional SNe Ia from Perlmutter et al. data. The dashed line is the prediction of OCDM with $\Omega_m = 0.2$ and $\Omega_\Lambda = 0$. The dotted line is the prediction of SCDM with $\Omega_m = 1$ and $\Omega_\Lambda = 0$. The two thick solid lines are predictions of Λ CDM, with $(\Omega_m, \Omega_\Lambda) = (0.3, 0.7)$, $(\Omega_m, \Omega_\Lambda) = (0.2, 0.8)$ respectively. The thin solid line is SCDM with $(1+z)$ dimming of SN Ia peak luminosity. (a) The distance modulus versus redshift.

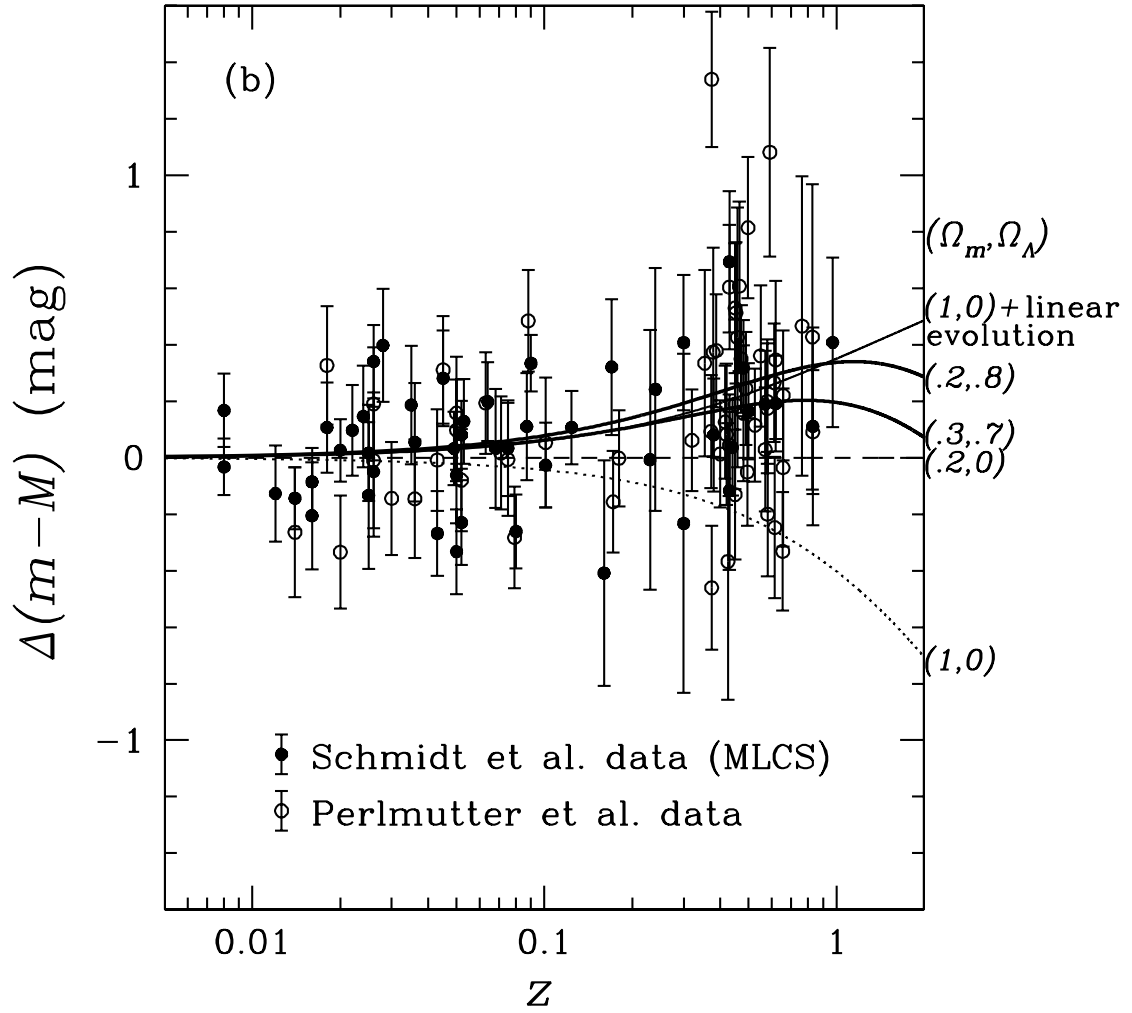


Fig. 3.— (b) The distance modulus relative to the prediction of the OCDM model.

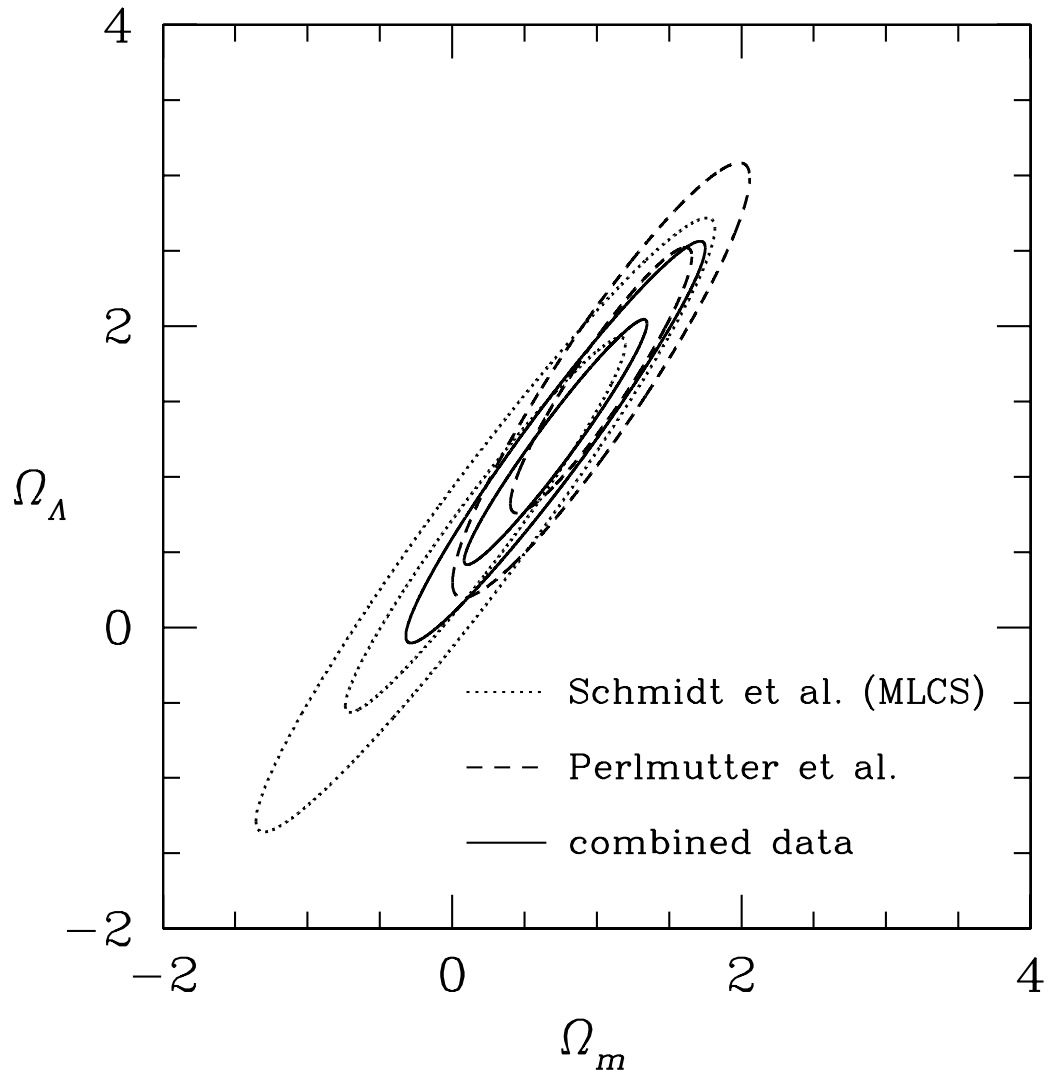


Fig. 4.— The 68.3% and 95.4% confidence contours in the $\Omega_\Lambda - \Omega_m$ plane. The dotted lines represent the Schmidt et al. data (50 SNe Ia), the dashed lines represent the Perlmutter et al. data (60 SNe Ia), and the solid lines represent the combined data (92 SNe Ia).

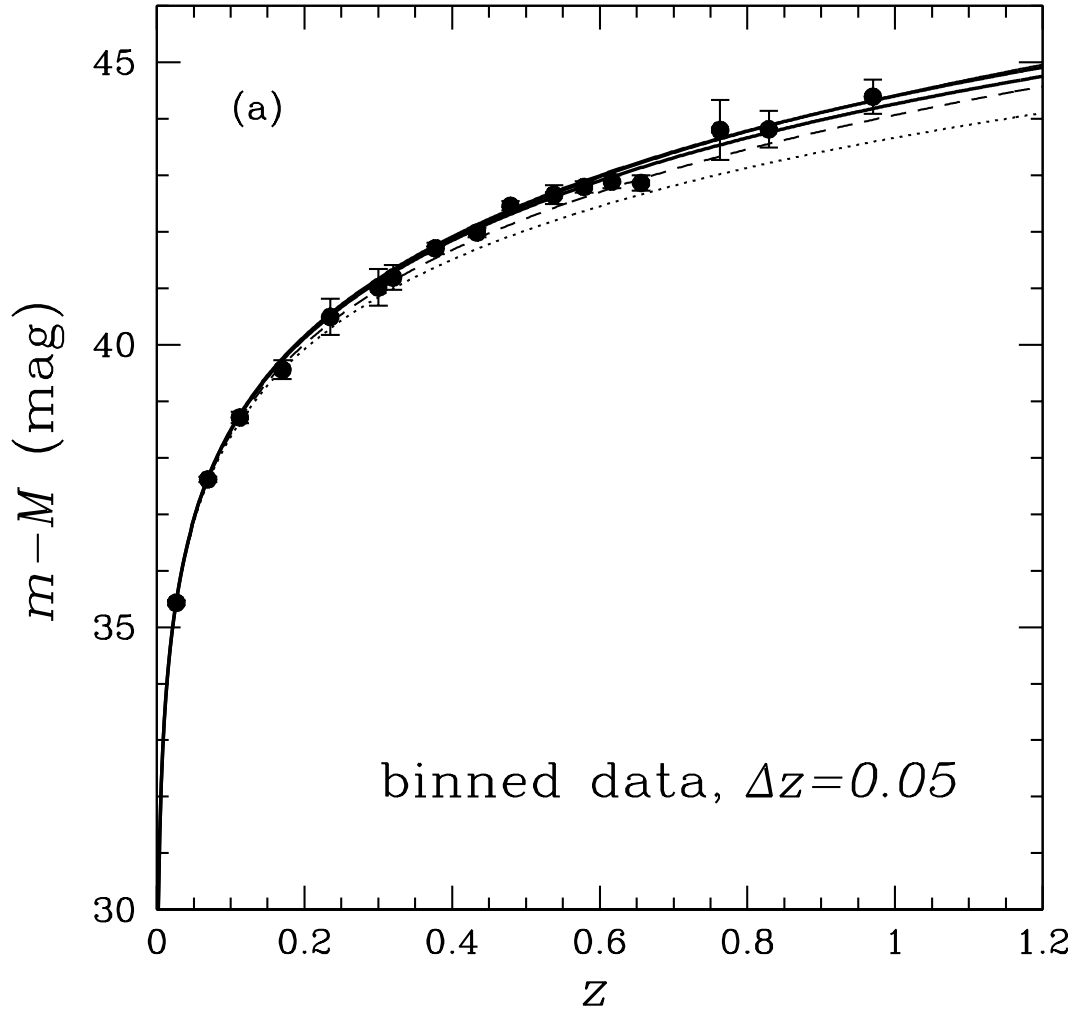


Fig. 5.— The magnitude-redshift plots of the binned data for 92 SNe Ia, with redshift bin $\Delta z = 0.05$. The line types are the same as in Fig.3. (a) The distance modulus versus redshift.

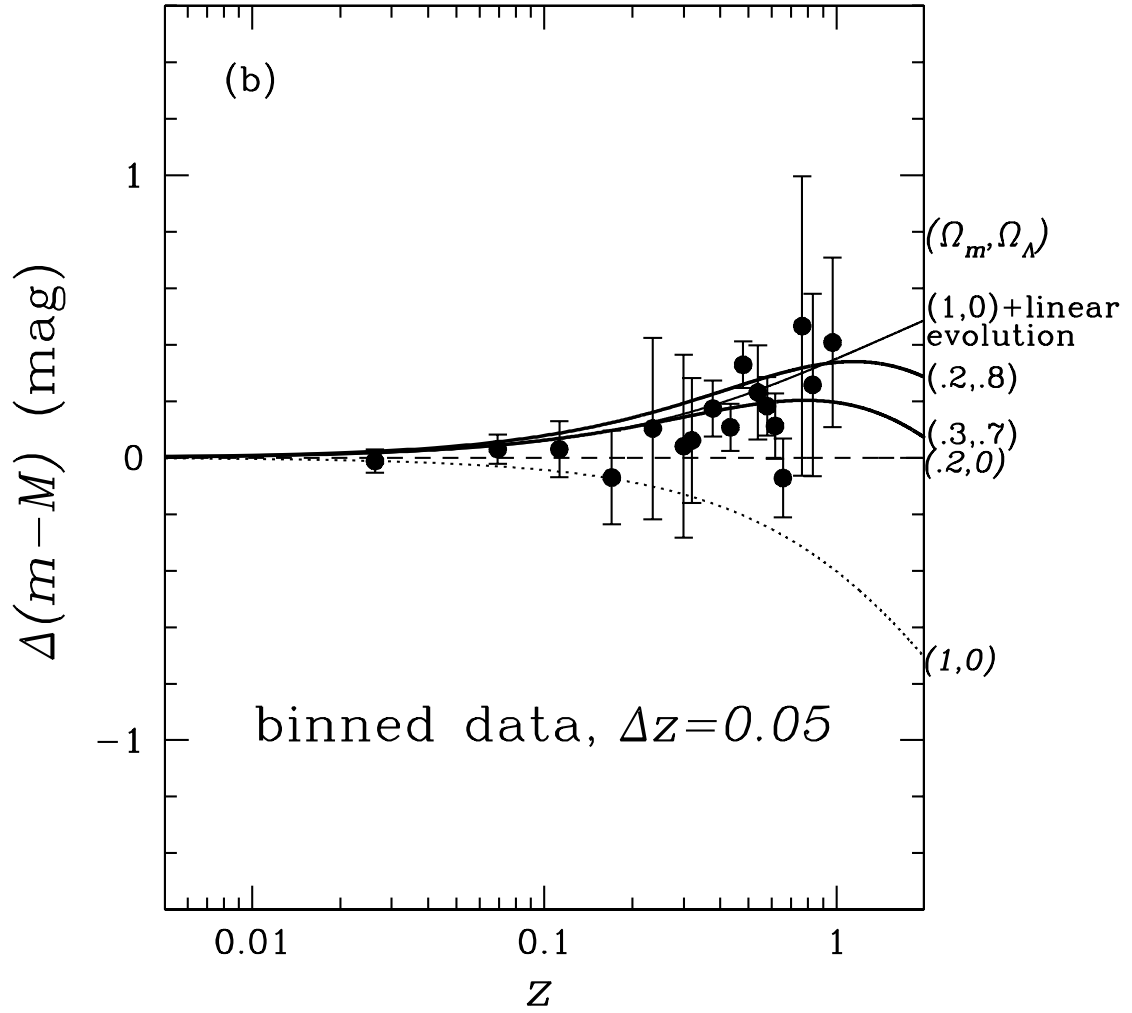


Fig. 5.— (b) The distance modulus relative to the prediction of the open cold dark matter model (OCDM) with $\Omega_m = 0.2$ and $\Omega_\Lambda = 0$.

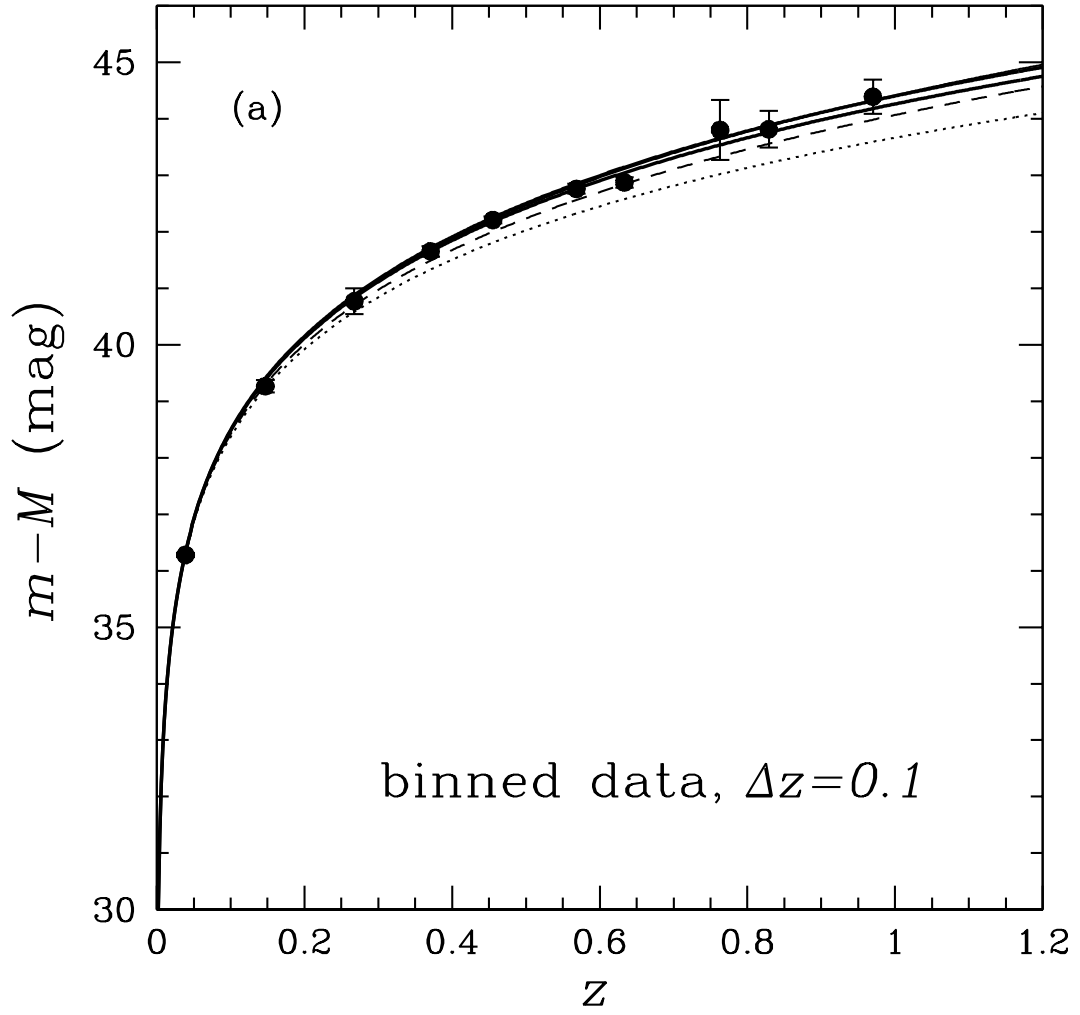


Fig. 6.— The same as Fig.5, but with redshift bin $\Delta z = 0.1$. (a) The distance modulus versus redshift.

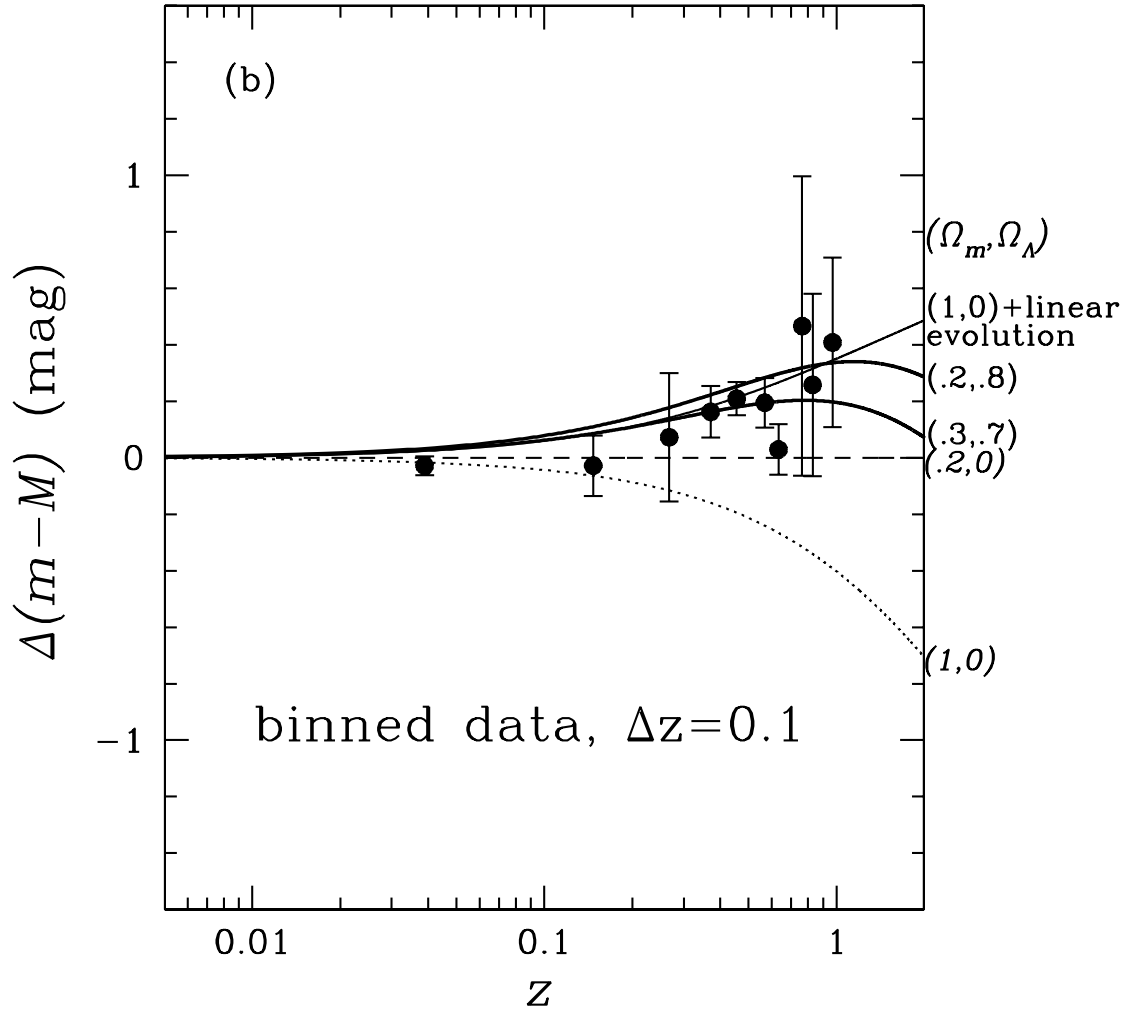


Fig. 6.— (b) The distance modulus relative to the prediction of the open cold dark matter model (OCDM) with $\Omega_m = 0.2$ and $\Omega_\Lambda = 0$.

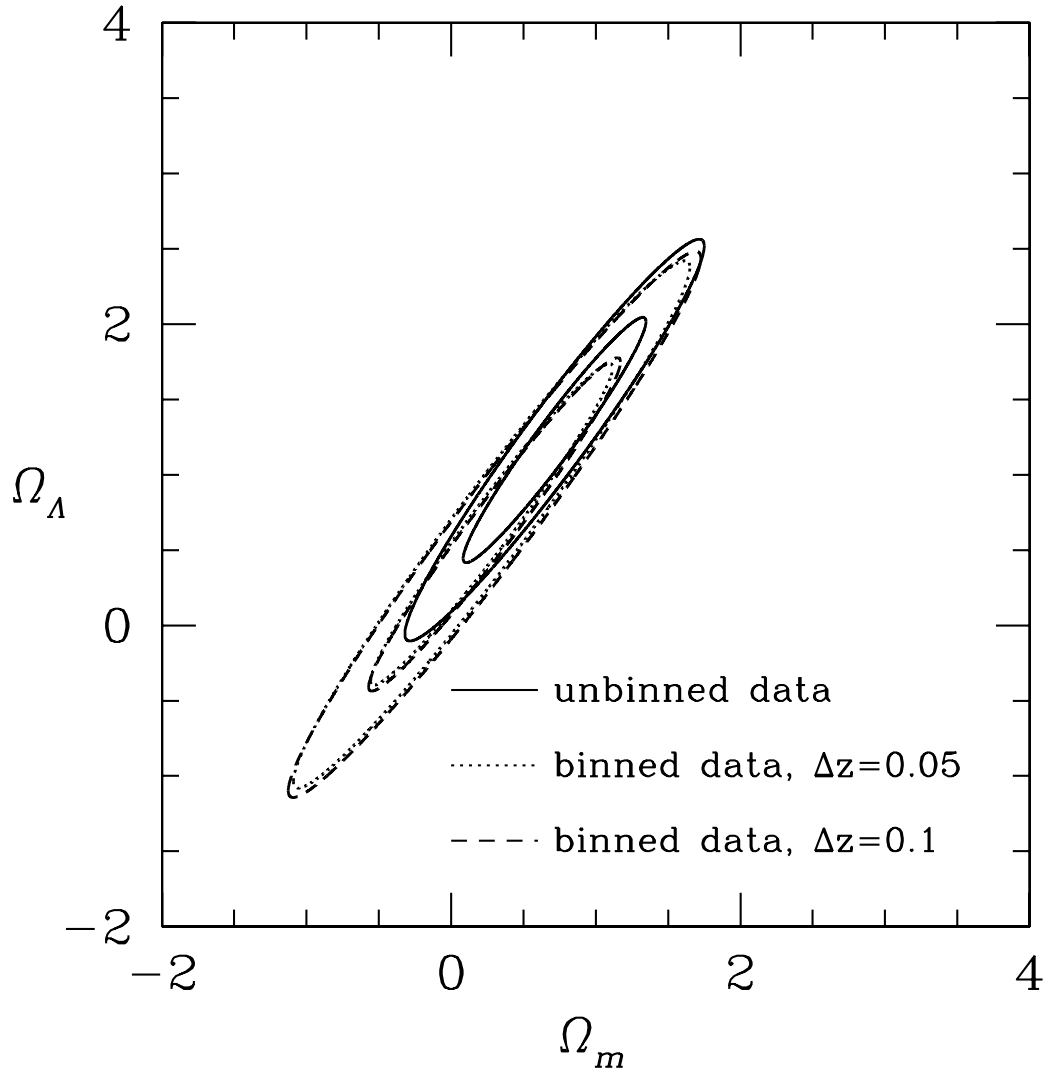


Fig. 7.— The 68.3% and 95.4% confidence contours in the $\Omega_\Lambda - \Omega_m$ plane. The solid lines represent the unbinned data, the dotted lines represent the binned data with redshift bin $\Delta z = 0.05$; the dashed lines represent the binned data with redshift bin $\Delta z = 0.1$.

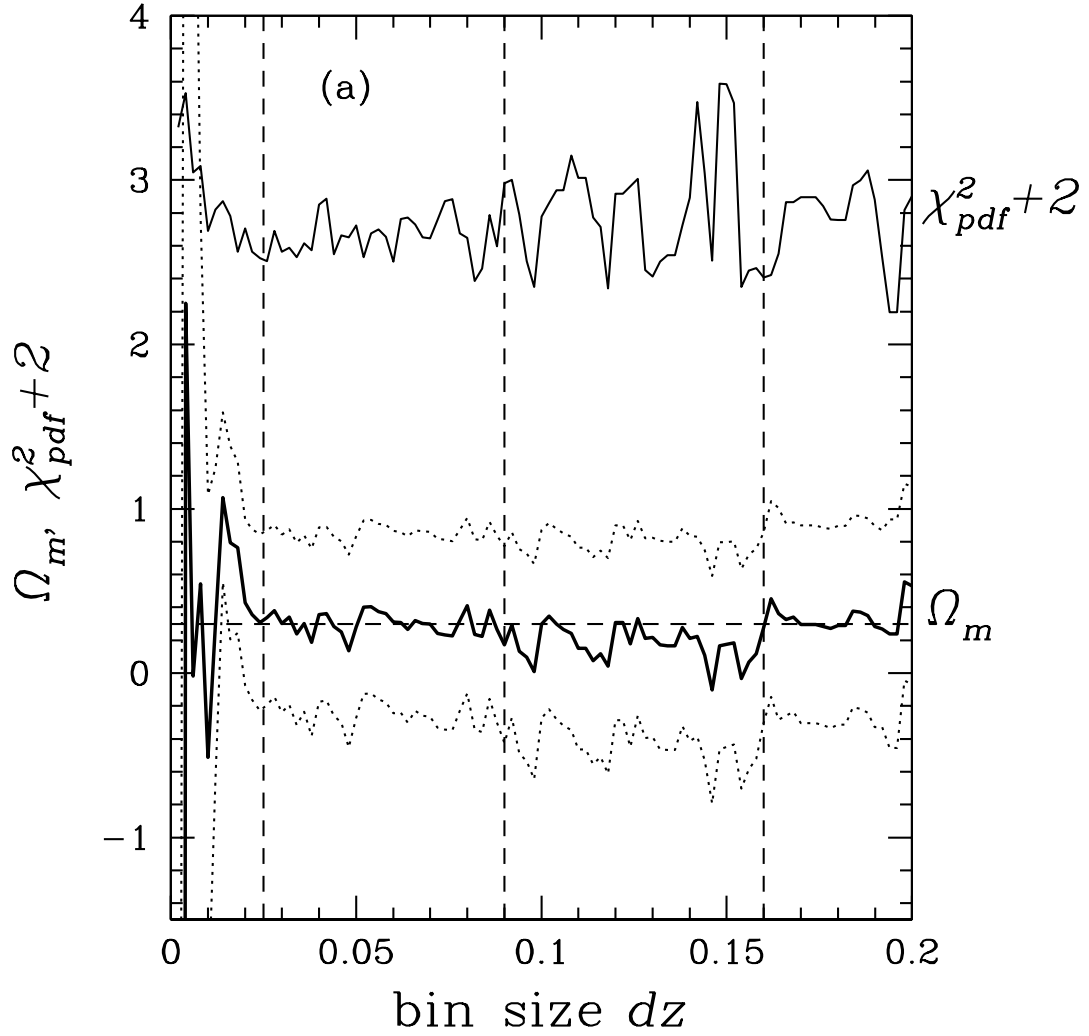


Fig. 8.— The estimated parameters from flux-averaged data as functions of the size of the redshift bin. The thick solid line is the estimated parameter, with 1σ errors marked by the dotted lines. The thin solid line is $\chi_{\nu}^2 + 2$. (a) Ω_m .

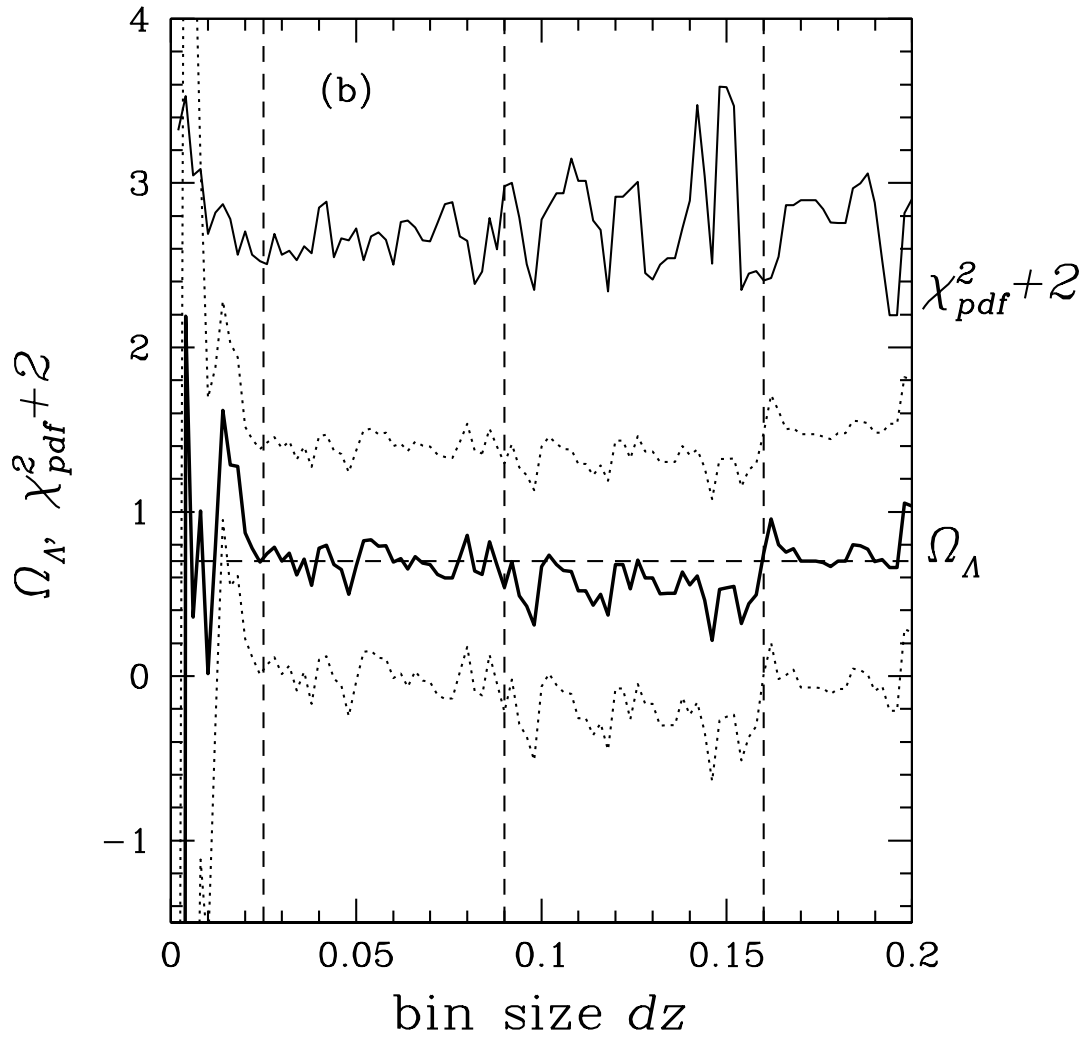


Fig. 8.— (b) Ω_Λ .